PROBLEMY MECHATRONIKI
UZBROJENIE, LOTNICTWO, INŻYNIERIA BEZPIECZEŃSTWA

ISSN 2081-5891

7, 4 (26), 2016, 115-130

PROBLEMS IN MECHATRONICS
ARMAMENT, AVIATION, SAFETY ENGINEERING

Numerical Investigation of the Wing-in-Ground Effect on Aerodynamic Characteristics

Stanisław WRZESIEŃ, Michał FRANT, Maciej MAJCHER*

Military University of Technology, Faculty of Mechatronics and Aerospace,
2 Sylwestra Kaliskiego Street, 00-908 Warsaw, Poland
**Corresponding author's e-mail address: maciej.majcher@wat.edu.pl*

Received by the editorial staff on 7 March 2016.
The reviewed and verified version was received on 6 June 2016.

DOI 10.5604/01.3001.0009.5022

Abstract: This paper presents the numerical evaluation of ground (proximity) effects on the basic aerodynamic characteristics of a specifically designed airplane model. The ground effects were investigated in relation to the angle of attack and flight altitude. The results were referenced to the characteristics of an object in motion unaffected by ground effects.
Keywords: mechanics, ground effect, aerodynamics, aerodynamic characteristics

1. INTRODUCTION

Aerodynamics usually involves flows around an isolated section, which could involve an entire aerofoil for example. This section condition is also referred to as "singular", which means that the flow velocity field of the section/aerofoil features no other objects.

However, engineering-critical circumstances exist under which the condition of isolation is not met, where flows occur around a set of sections.

The most important problems of this kind include section palisade flows, and flows around a section or an aerofoil in the direct proximity of a plane. The latter case includes the flow phenomena occurring near the ground, known as the "wing-in-ground" effect (or WIG effect).

This type of flow leads to issues related to qualitative and quantitative ground effects on the aerodynamic characteristics determined for an isolated, or singular aerofoil. The relations defining the WIG effect apply during take-off and landing of every aircraft, as well as during the operation of ram-wing craft or ekranoplans (known as WIG effect craft for short).

The WIG effect was discovered in the 1920s [6], [8], [12], when its impact was observed on the aerodynamic characteristics of aircraft. The WIG effect specifically applies to changes in the lift coefficient of wings, while another important WIG effect is the change in the total drag coefficient. Changes in the lift and drag coefficients affect the lift to drag (L/D) ratio of any flying object.

Any investigation into the WIG effect, especially in objects having complex geometrical forms, is very difficult. Some analytical research has been undertaken involving rectilinear aerofoil sections using the "mirror reflection method" [6], suggesting that lift increases near the ground, a conclusion confirmed in numerous experiments. However, analytical methods do not allow evaluation of the changes in drag.

Given the feasibility of applying CFD-based simulation techniques, this work attempted to investigate the problem of evaluating drag changes using numerical calculation methods. A simplified 3D model of an aircraft body was used without the usual details associated with an actual aircraft body. A virtualized aircraft body enables a qualitative and quantitative evaluation of the WIG effect on the aerodynamic properties. However, a model of this kind cannot be used to determine an optimum flight altitude with the best utilization of the WIG effect and uncompromised flight safety.

Known WIG effect designs are usually divided into three classes [6], [7], [12]:

- Class A: WIG effect craft that directly use the ground effect and fly directly over the ground surface.
- Class B: WIG effect craft capable of temporary flight at zero WIG effect altitudes with a maximum altitude limit of 150 metres.
- Class C: WIG effect craft capable of flight at altitudes exceeding 150 metres.

Not unlike typical aircraft, the main lifting component of a WIG effect craft are aerofoils designed to achieve a good pressure distribution that results in a certain lift coefficient value.

The ground effect changes the pressure distribution around the aerofoil, which results in a different lift coefficient to that of the isolated aerofoil lift coefficient. The qualitative pressure changes are shown in Fig. 1.

The effects of this include a change in the take-off and landing distances by as much as 20% from the take-off distance determined without the WIG effect [13].

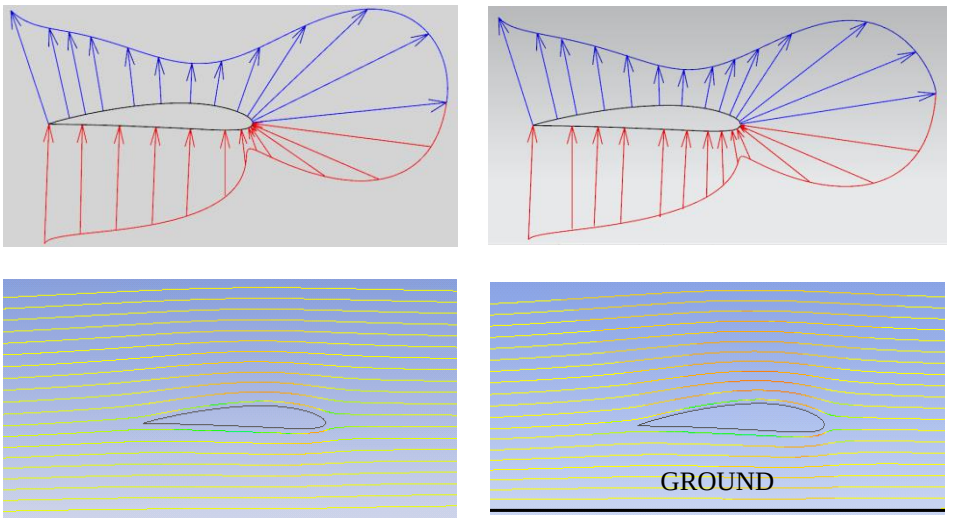

Fig. 1. Flow around an isolated section vs. WIG effect section

The investigations into aircraft sections [2-3] and aerofoils [4] unanimously state that the WIG effect significantly changes the following aerodynamic characteristics of an aircraft:

- lift is increased at the same angle of attack;
- wing and elevator induced drag is reduced;
- power required to fly is reduced.

The available references do not provide quantitative relations between the proximity of the ground and the aerodynamic characteristics that would be helpful in the design engineering of aerodynamic bodies employing the WIG effect during take-off and landing, the two most dangerous stages of flight.

2. NUMERICAL AND WIND TUNNEL MODELS. TEST RESULTS

An aerodynamic body system was developed with the guidelines of [5] and [10] to test the ground effect on the aerodynamic characteristics.

These references include algorithms for conventional model solutions, while certain modifications were introduced to the relations to deliver a body design that featured mass and geometry parameters comparable to actual aircraft models. Therefore, a virtual model of an aircraft was built in NX 7.5, a CAD suite.

The aircraft body model is shown in Fig. 2 [9]. Table 1 lists the main geometrical parameters of the virtual aircraft model.

Table 1. Main geometrical parameters of the 3D aircraft model [9]

Parameter	Designation	Units	Value
Aerofoil	NACA 4412	-	-
Wing area	S	m^2	25.76
Wing aspect ratio	λ	-	3
Wing convergence	η	-	0.5
Wingspan	l	m	8.79
Root chord	b_{Root}	m	3.91
Tip chord	b_{Tip}	m	1.95
Mean aerodynamic chord	b_{MAC}	m	3.04
Position of MAC along the wing	Y_{FMC}	m	1.95

The virtual aircraft model was then adjusted to suit the numerical calculations, which was achieved by simplifying the small edges and surfaces of the 3D body that would otherwise make the numeric mesh difficult or impossible to build. Further simplification entailed removal of the engine nacelles and wing floats.

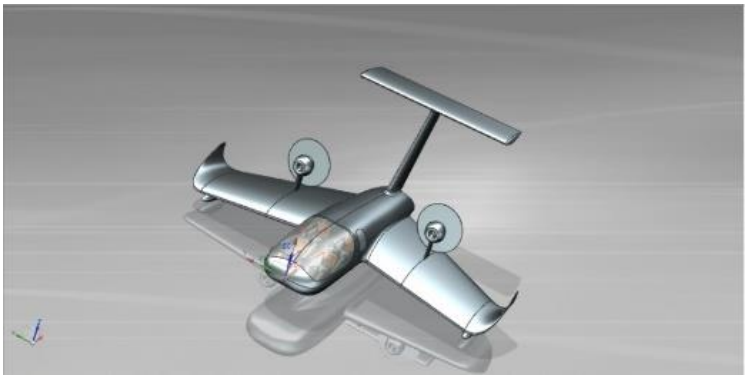

Fig. 2. 3D model of the designed aerodynamic body [9]

The simplified 3D model had a computational surface area in the form of a rectangular prism with a height of 210 [m] and a square base with a 140 [m] side. To simulate the WIG effect, the computational surface area was restricted to a horizontal plane the position of which was defined by the flight conditions at a specific altitude.

The numerical calculations considered the horizontal plane to be a moving wall with a velocity corresponding to the assumed cruising speed. The other boundaries of the computational surface area were pre-set with pressure far field conditions.

A hybrid mesh was built for the computational surface area using the Mesh Ansys Fluent module. The 3D model surfaces were transformed into a triangular mesh with prismatic components within the boundary layer areas (Fig. 3) and a tetrahedral mesh for all other areas of the model.

This was a compromise solution, one suitable for objects having complex geometry. The quality of the resulting computational mesh was verified [1].

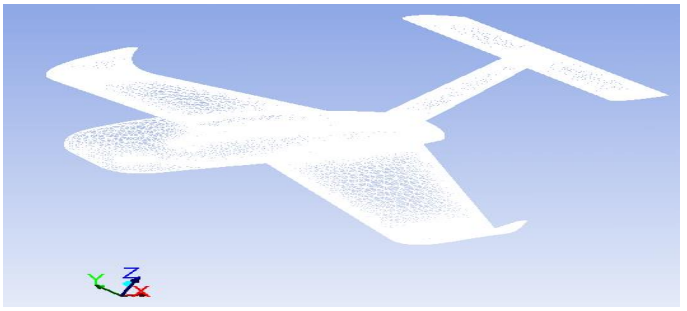

Fig. 3. View of the mesh imposed on the 3D model surface

To verify the numerical calculations, a wind tunnel model was built to obtain comparable results from physical testing. The model scale chosen was 1:16, whereas the experimental test cycle was completed with a flow rate of approx. 28 m/s, at a Reynolds number (Re) of $3.46 \cdot 10^5$.

Fig. 4. Actual model suspended in the wind tunnel [9]

The experimental results were compared with the numerical results, with identical aerodynamic flow conditions being assumed in each case.

The numerical calculations used the following pre-sets:

- Solver: Density-Based
- Turbulence model: Spalart-Almaras
- Mach number (Ma): 0.139.

The numerical results are shown in Figs. 5 and 6, and show a good qualitative and quantitative agreement between the resulting characteristics. This agreement of the results indicates that the designed computational mesh and the turbulence model were both correct. Hence, the mesh parameters and turbulence model were applied in subsequent variants of the numerical testing.

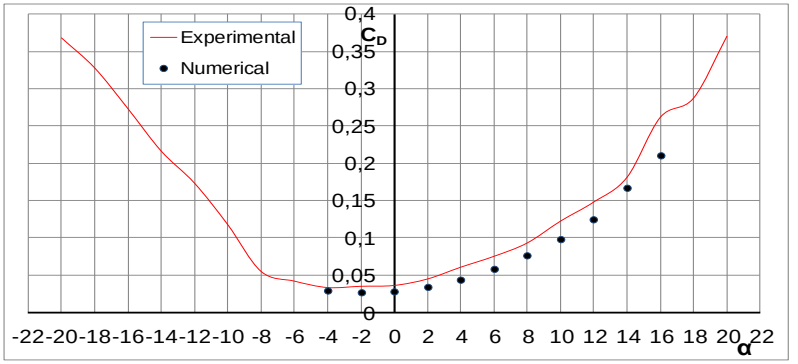

Fig. 5. Drag coefficient C_D vs. angle of attack α, for the numerically and experimentally tested model [9]

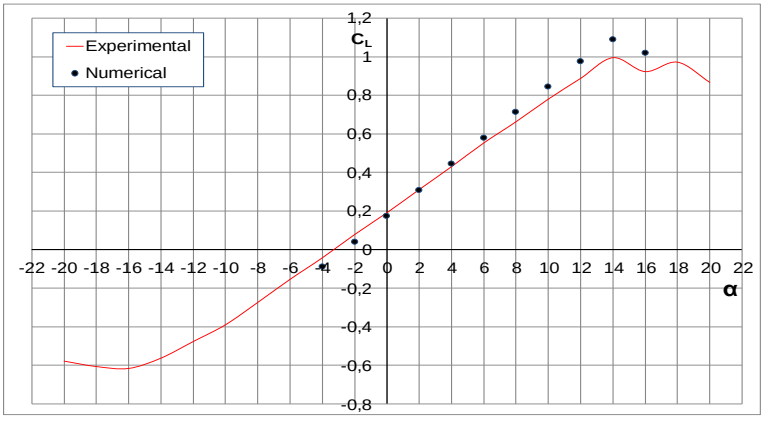

Fig. 6. Lift coefficient C_L vs. angle of attack α, for the numerically and experimentally tested model [9]

Note that the results shown above apply to conditions without ground effect and were generated to verify the numerical method.

The wind tunnel experiments did not emulate flight with the WIG effect due to certain technical difficulties caused by the design of the aerodynamic balance. The model is fixed in place with piano strings, which prevents the use of a flat panel to simulate the ground proximity effect. It was decided to do the experiments without the WIG effect and to verify the numerical method involving specific operations on the computational meshes, applying a specific turbulence model, etc.

Also note that ground proximity in the simulations only requires modification of the boundary conditions for the model in question.

3. NUMERICAL DETERMINATION OF THE GROUND EFFECT ON AERODYNAMIC CHARACTERISTICS

This section presents the numerical results of testing a 1 : 1 scale 3D virtual object with ground effect.

The calculation process was run at three angle of attack values, 0 [deg], 1 [deg], and 2 [deg], at flight altitudes of 1 [m], 1.25 [m], 1.5 [m], 1.75 [m], and 2 [m]. The small angle of attack values were imposed by the specific flight model of WIG effect craft, as an aircraft of this type flies only at low angles of attack. A specific calculation case was input to prepare the models for numerical simulations. 'WIG' denotes an analysis with the WIG effect included, the number in metres denotes the flight altitude in metres, and the last digit is the angle of attack. For example: WIG_1.25m_1 is a calculation based on the WIG effect simulated at an altitude of 1.25 [m] and an angle of attack of 1 [deg]. Figs. 7 to 11 give examples of the static pressure distribution for a selected wing section, at various flight altitudes and a fixed angle of attack.

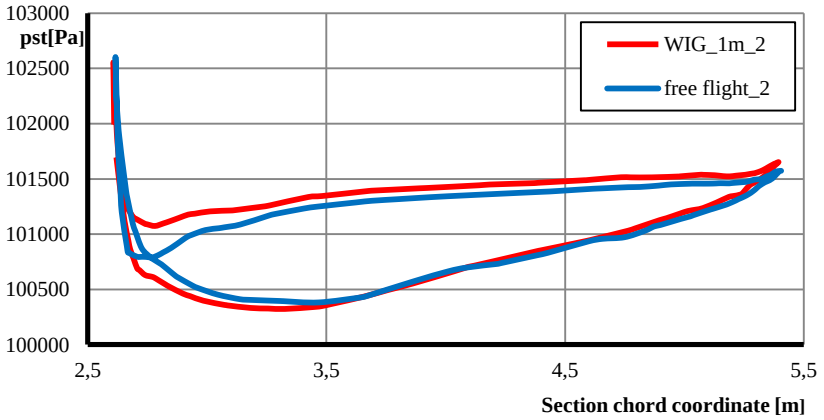

Fig. 7. Static pressure distribution at a section 2.5 [m] away from the airplane axis of symmetry, altitude: 1 [m], angle of attack: 2 [deg]

The figures show that with a fixed angle of attack, the field delimited by the static pressure distribution varied with the flight altitude.

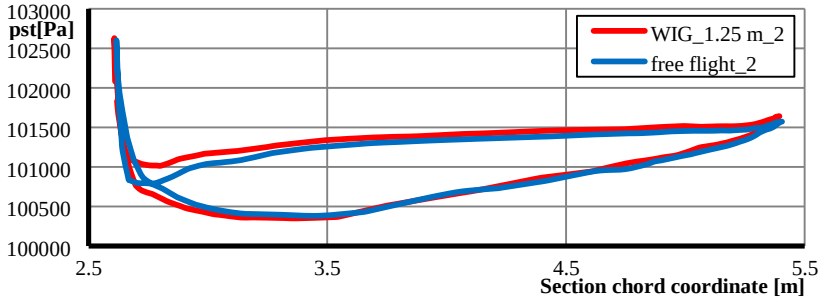

Fig. 8. Static pressure distribution at a section 2.5 [m] away from the airplane axis of symmetry, altitude: 1.25 [m], angle of attack: 2 [deg]

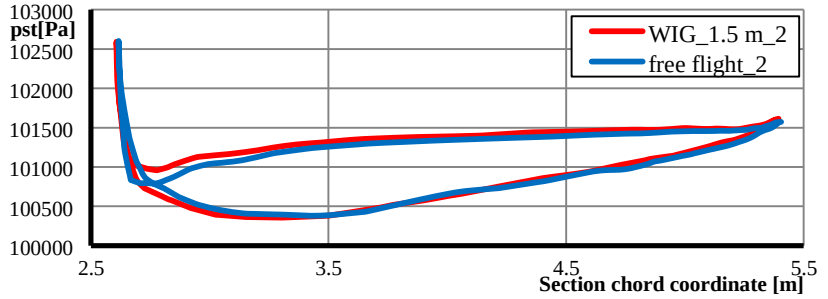

Fig. 9. Static pressure distribution at a section 2.5 [m] away from the airplane axis of symmetry, altitude: 1.5 [m], angle of attack: 2 [deg]

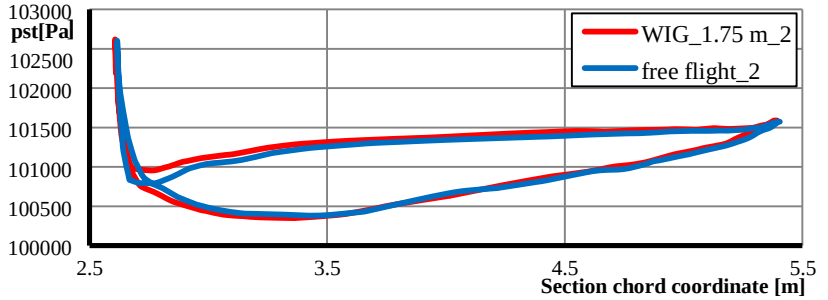

Fig. 10. Static pressure distribution at a section 2.5 [m] away from the airplane axis of symmetry, altitude: 1.75 [m], angle of attack: 2 [deg]

These changes increased the lift. For the sake of comparison, the pressure distribution is also shown without the WIG effect, and it is evident that, in each case, the static pressure distribution with the WIG effect clearly differed from the pressure distribution in free flight. This difference increased in inverse proportion to the distance from the ground. The largest changes in the static pressure distribution were observed at the leading edge.

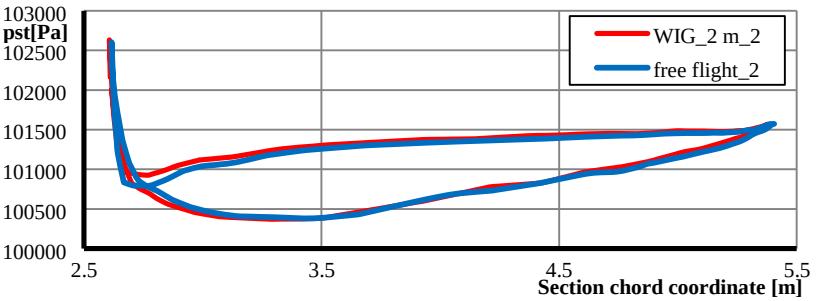

Fig. 11. Static pressure distribution at a section 2.5 [m] away from the airplane axis of symmetry, altitude: 2 [m], angle of attack: 2 [deg]

The effects of the angle of attack were also tested for specific cases of flight. Figs. 12 to 14 show examples of static pressure distribution at a selected wing section, at a fixed flight altitude and various angles of attack. The figures show that with a fixed flight altitude, the field delimited by the static pressure distribution varied with the angle of attack. The largest changes were observed around the leading edge. These changes increased the lift, while the static pressure distribution difference increased proportionally to the angle of attack.

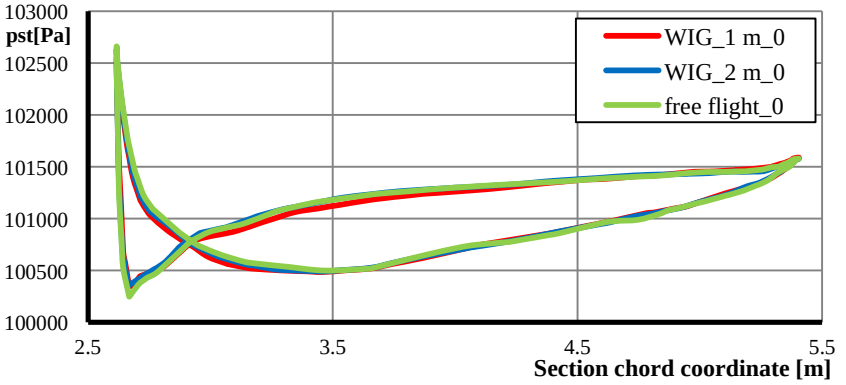

Fig. 12. Static pressure distribution at a section 2.5 [m] away from the airplane axis of symmetry, angle of attack: 0 [deg]

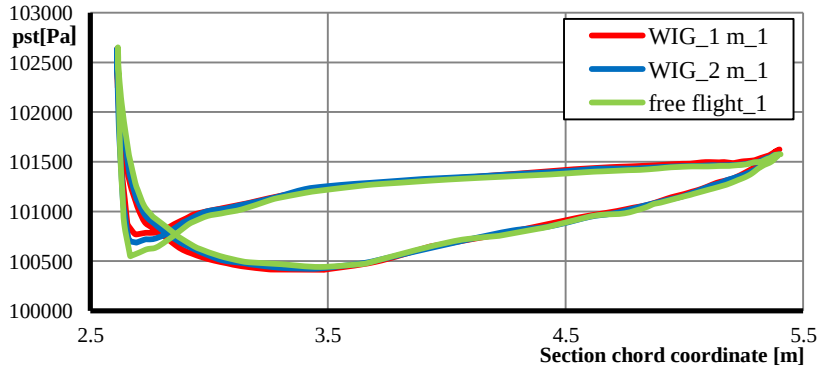

Fig. 13. Static pressure distribution at a section 2.5 [m] away from the airplane axis of symmetry, angle of attack: 1 [deg]

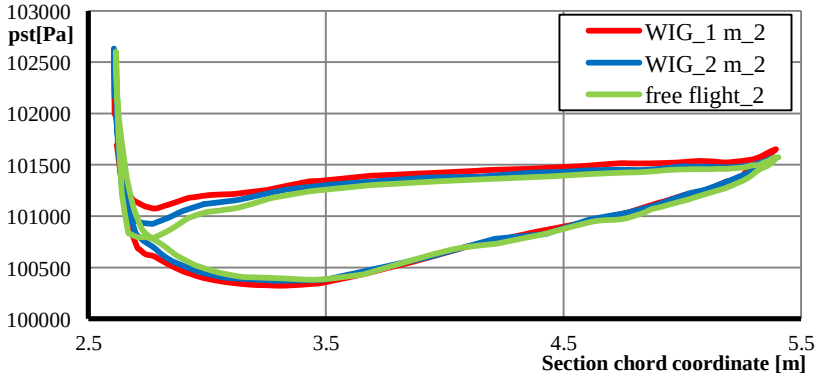

Fig. 14. Static pressure distribution at a section 2.5 [m] away from the airplane axis of symmetry, angle of attack: 2 [deg]

Figs. 15 to 17 show the lift coefficient values, the drag coefficient values, and the L/D values at various angles of attack as a function of flight altitude with the WIG effect. These show that when the angle of attack increased, the lift coefficient C_L also increased. The actual lift coefficient value depended on the angle of attack when the flight altitude increased. When the angle of attack was $\alpha = 0$ [deg], increasing the flight altitude increased the lift coefficient C_L; when the angle of attack was $\alpha = 1$ [deg], changes in the flight altitude did not affect the lift coefficient C_L, whereas at $\alpha = 2$ [deg], reducing the flight altitude reduced the lift coefficient C_L.

The highest lift coefficient value was observed at a flight altitude of 1 [m] with an angle of attack of $\alpha = 2$ [deg]; the lowest lift coefficient value was found at a flight altitude of 1 [m] and an angle of attack of $\alpha = 0$ [deg].

When the angle of attack increased, the drag coefficient C_D also increased. At an angle of attack of α = 0 [deg], the drag coefficient C_D increased between flight altitudes of 1 and 1.25 [m]; however, the drag coefficient value did not change markedly at higher altitudes.

At α = 1 [deg], the drag coefficient C_D increased up to H = 1.75 [m], whereas at α = 2 [deg], C_D increased over the entire flight altitude range. The changes in C_L and C_D caused significant changes in the L/D and α (Fig. 17). It was clear that if α = 0 [deg], the L/D was first reduced (up to H = 1.25 [m]), and then the L/D increased. At α = 1 [deg], the effect of flight altitude on the L/D was minor; α = 2 [deg] markedly reducing the L/D value. This effect is as expected: as the flight altitude increases, the WIG effect reduces.

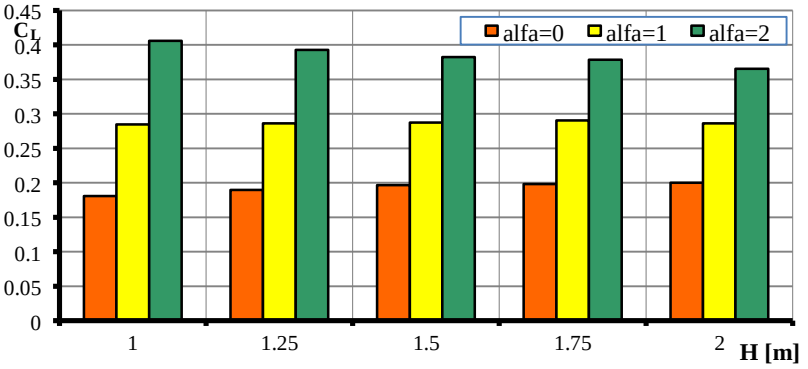

Fig. 15. Lift coefficient distribution vs. flight altitude at various angles of attack

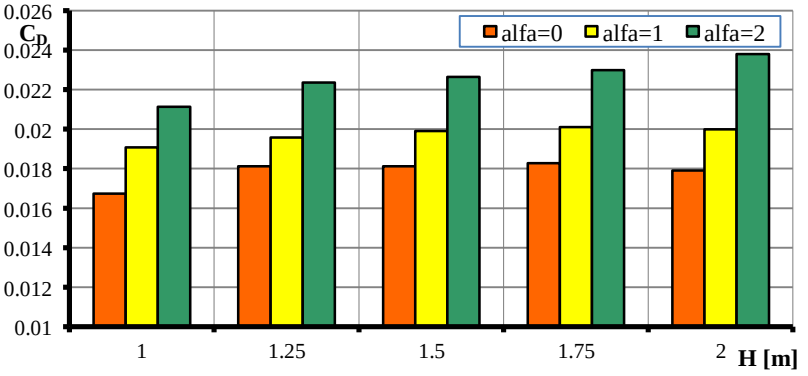

Fig. 16. Drag coefficient distribution vs. flight altitude at various angles of attack

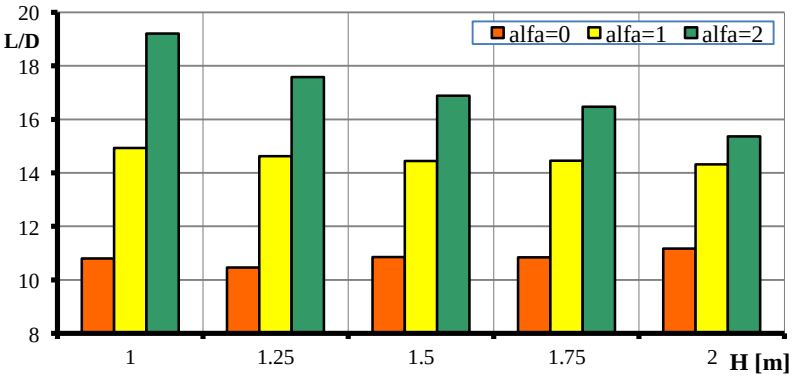

Fig. 17. *L*/*D* distribution vs. flight altitude at various angles of attack

Figs. 18 to 20 show the WIG effect in comparison to free flight conditions. Fig. 18 shows changes in the lift coefficient. Fig. 19 shows changes in the drag coefficient. Fig. 20 shows changes in the *L*/*D*.

To sum up, the WIG effect increased the lift coefficient and reduced the drag coefficient, and these changes improved the *L*/*D* ratio of the aircraft.

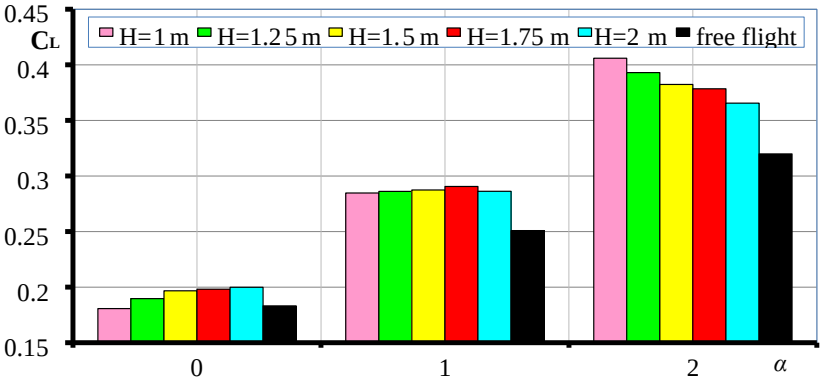

Fig. 18. Relationship between the lift coefficient and the angle of attack at various flight altitudes

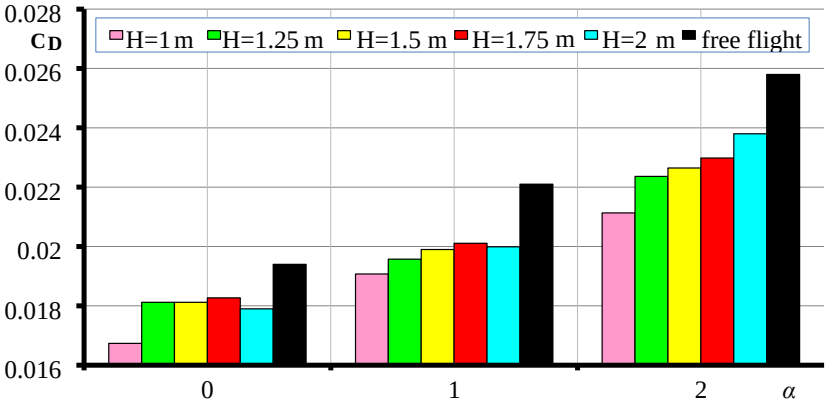

Fig. 19. Relationship between the drag coefficient and the angle of attack at various flight altitudes

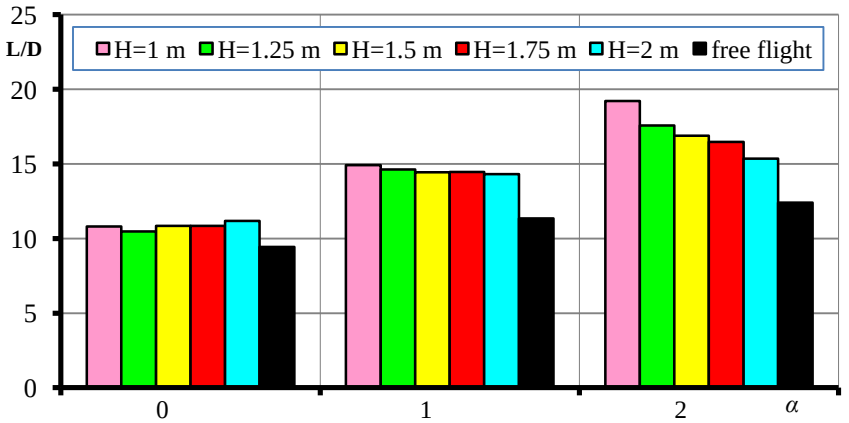

Fig. 20. Relationship between the *L*/*D* and the angle of attack at various flight altitudes

4. CONCLUSIONS

This work investigated the WIG effect using a numerical method, the results of which were verified using an experimental method. There was good agreement between the results of each method (see Figs. 5 and 6), which justified the application of numerical simulation and analysis for complex instances of flows around bodies. The numerical results were fully compliant with the generally understood wing-in-ground effect phenomena.

To conclude, the application of numerical simulation with an advanced CFD package is justified as a method of solving atypical research problems. However, a precondition to achieving acceptable results exists: great experience in the application of these numerical methods, and thorough understanding of the physical aspects of the studied phenomena.

REFERENCES

[1] ANSYS Meshing User Guide. Release 15 November 2013.
[2] Abramowski Tomasz. 2007. "Numerical investigation of aerofoil in ground proximity". *Journal of Theoretical and Applied Mechanics* 45 (2): 425-436.
[3] Carter Arthur. 1961. *Effect of Ground Proximity on the Aerodynamic Characteristics of AR 1 Aerofoils With and Without End Plates*. NASA TN D-970.
[4] Carter Arthur. 1970. *Effects of Ground Proximity on the Longitudinal Aerodynamic Characteristics of an Unswept AR 10 Wing*, NASA TN D-5662.
[5] Danilecki Stanisław. 2006. *Projektowanie samolotów*. Wrocław: Oficyna Wydawnicza Politechniki Wrocławskiej.
[6] Halloran Michael, Sean O'Maera. 1999. *Wing in Ground Effect Craft Review*. Melbourne: Defence Science & Technology Organization Aeronautical and Maritime Research Laboratory.
[7] Hansen Eric. 2011. *Hovercraft Wing-In-Ground (WIG)*. Norfolk: Platform Research, Combatant Craft Division.
[8] Hooker Stephen. 1989. "A Review of Current Technical Knowledge Necessary to Develop Large Scale Wing-In-Surface Effect Craft", *AIAA Paper* 89-1497.
[9] Majcher Maciej. 2013. *Projekt wstępny samolotu do lotów na małych wysokościach*. master thesis. Warsaw: Military University of Technology.
[10] Raymer Daniel. 1992. *Aircraft Design: A Conceptual Approach*. Washington: American Institute of Aeronautics and Astronautics.
[11] Rożdestvenskij Kirill. 2006. "Wing-in-ground effect vehicles". *Progress in Aerospace Sciences* 42 (3) : 211-283.
[12] Seuret Dominique, Christoph Wangler. 2005. "Construction of a Low Cost Wing-In-Ground Effect Craft" (*online*).
[13] Wnuk Łukasz. *Wpływ bliskości ziemi na charakterystyki aerodynamiczne samolotu*. Final seminary 2001/2002. Rzeszów University of Technology.

Numeryczne badania wpływu efektu przypowierzchniowego na charakterystyki aerodynamiczne

Stanisław WRZESIEŃ, Michał FRANT, Maciej MAJCHER

Streszczenie. W pracy przedstawiono badania numeryczne wpływu efektu bliskości ziemi na podstawowe charakterystyki aerodynamiczne specjalnie do tego celu zaprojektowanej bryły samolotu. Zbadano wpływ bliskości ziemi w zależności od kąta natarcia oraz w zależności od wysokości lotu. Wyniki odniesiono do charakterystyk obiektu poruszającego się bez efektu bliskości ziemi.
Słowa kluczowe: efekt bliskości ziemi, aerodynamika, charakterystyki aerodynamiczne